Dalton
Transactions

Cite this: *Dalton Trans.*, 2011, **40**, 4527

www.rsc.org/dalton

PAPER

Ag(I) and Zn(II) coordination polymers with a bulky naphthalene-based dicarboxyl tecton and different 4,4′-bipyridyl-like bridging co-ligands: structural regulation and properties†

Shao-Ming Fang,[a] Min Hu,[a] Qiang Zhang,[a] Miao Du*[b] and Chun-Sen Liu*[a]

Received 23rd July 2010, Accepted 8th February 2011
DOI: 10.1039/c0dt00903b

A series of six Ag(I) and Zn(II) coordination polymers, namely, $[\mathrm{Ag_2}(\mathbf{ndc})]_\infty$ (**1**), $\{[\mathrm{Zn}(\mathbf{ndc})(\mathrm{H_2O})](\mathrm{H_2O})\}_\infty$ (**2**), $\{[\mathrm{Ag_2}(\mathbf{ndc})(\mathrm{4bpy})_2][\mathrm{Ag}(\mathrm{4bpy})(\mathrm{H_2O})](\mathrm{ClO_4})(\mathrm{H_2O})_2\}_\infty$ (**3**), $[\mathrm{Zn_5}(\mathbf{ndc})_4(\mathrm{4bpy})_2(\mu_3\text{-}\mathrm{OH})_2]_\infty$ (**4**), $\{[\mathrm{Ag}(\mathbf{ndc})(\mathrm{abp})][\mathrm{Ag}(\mathrm{abp})](\mathrm{H_2O})_3\}_\infty$ (**5**), and $\{[\mathrm{Zn_2}(\mathbf{ndc})_2(\mathrm{abp})(\mathrm{H_2O})_2](\mathrm{H_2O})_2\}_\infty$ (**6**), have been prepared by using 2,3-naphthalenedicarboxylic acid (H$_2$**ndc**), an analogue of 1,2-benzenedicarboxylic acid (H$_2$**bdc**), and different 4,4′-bipyridyl-like bridging co-ligands 4,4′-bipyridine (4bpy) and *trans*-4,4′-azobis(pyridine) (abp). The initial complexes **1** and **2** display the unusual two-dimensional (2-D) five-connected (4^8.6^2) and the 2-D three-connected (4.8^2) coordination networks, respectively. When two comparable rod-like linkers 4bpy and abp (with different *N*,*N*′-donor separations of the molecular backbones of *ca.* 7 and 9 Å) are further introduced, two one-dimensional (1-D) complexes **3** and **5**, a three-dimensional (3-D) coordination framework **4** with (4^3)(4^3.6^3)(4^3.6^5.8^2)(4^4.6^4.8^2)(4^{10}.6^5) topology and a 2-D 6^3 layered coordination polymer **6** are constructed. A structural comparison of these complexes with those based on the structurally related **bdc** ligand suggests that the extended π-conjugated system of **ndc** with different electronic nature and steric bulk play an important role in constructing the supramolecular architectures for **1–6**, which are also regulated by different bridging *N*-donor co-ligands and metal ions. Moreover, complexes **1–6** show strong solid-state luminescence emissions at room temperature that mainly originate from the intraligand transitions of **ndc**.

Introduction

In recent years, d^{10} metal–organic coordination architectures have attracted great interest due to not only their structural diversity but also their potential applications as functional materials.[1,2] In this field, several strategies have been developed to achieve the controllable assembly of such crystalline systems with desired structures and properties,[3] among which the appropriate choice of well-designed organic ligands as bridges or terminal groups, and metal ions or clusters as nodes is one of the most effective candidates.[4]

As for the organic ligands, versatile carboxyl compounds, especially aromatic carboxylic acids, such as 1,2-benzenedicarboxylic acid,[5,6] 1,3-benzenedicarboxylic acid,[7] 1,4-benzenedicarboxylic acid,[8] 1,3,5-benzenetricarboxylic acid,[9] and 1,2,4,5-benzenetetracarboxylic acid,[10] have been extensively used in the preparation of various metal-carboxylate complexes owing to their rich coordination modes. To investigate the influence of bulky aromatic skeletons of such ligands on structures and properties of their coordination complexes, large aromatic systems such as anthracene-9-carboxylic acid,[11] anthracene-9,10-dicarboxylic acid,[12] anthracene-2,3,6,7-tetracarboxylic acid,[3d] and perylene-3,4,9,10-tetracarboxylic acid[12h] have been used by us and others to construct a series of 3d- and 4f-block metal complexes, which show diverse discrete (dinuclear, tetranuclear, pentanuclear, or hexanuclear) and infinite (1-D, 2-D, or 3-D) structures as well as interesting magnetic and luminescent properties. As such, the naphthalene-based di- and multi-carboxyl ligands, such as 1,4-[13] and 2,6-naphthalenedicarboxylic[14] as well as 1,4,5,8-naphthalenetetracarboxylic[15] acids, have also been successfully employed to prepare coordination complexes. Despite the remarkable achievements in this aspect,[1–15] to predict and further accurately control the framework array of a given target still remains a considerable challenge at this stage. This mainly arises from the fact that the assembled progress may be influenced by many

---

[a] *Zhengzhou University of Light Industry, Henan Provincial Key Laboratory of Surface & Interface Science, Zhengzhou, Henan, 450002, P. R. China. E-mail: chunsenliu@zzuli.edu.cn*
[b] *College of Chemistry, Tianjin Key Laboratory of Structure and Performance for Functional Molecule, Tianjin Normal University, Tianjin, 300387, P. R. China. E-mail: dumiao@public.tpt.tj.cn*

† Electronic supplementary information (ESI) available: Additional structural figures (Figs S1–S14), TG curves (Fig. S16), and PXRD patterns (Fig. S17) for complexes **1–6**. Solid state excitation/emission spectra of naphthalene-2,3-dicarboxylic acid (H$_2$**ndc**) as well as the auxiliary co-ligands 4,4′-bipyridine (4bpy) and *trans*-4,4′-azobis(pyridine) (abp) at room temperature (Fig. S15). Selected bond distances and angles for **1–6** (Tables S1–S6). CCDC reference numbers 783375, 761951, 783376, 761953, 783377, and 761954 for **1–6**. For ESI and crystallographic data in CIF or other electronic format see DOI: 10.1039/c0dt00903b

intrinsic and external parameters, which will determine the formation of different thermodynamically favored crystalline products. For instance, the skilful introduction of 4,4′-bipyridyl-like bridging co-ligands into such reaction systems usually results in completely different coordination architectures.[1b] In this regard, an analysis of the Cambridge Structural Database (CSD) reveals only one mononuclear Cu(II) complex [Cu(trpy)(**ndc**)(H_2O)] involving 2,3-naphthalenedicarboxylate (**ndc**) and 2,2′:6′2″-terpyridine (trpy) has been reported.[16] Thus, further efforts are required to provide more information on the coordination behavior of **ndc**, in order to design and prepare new crystalline materials with such types of organic ligands.

Considering all the above-mentioned aspects, two kinds of pre-designed building blocks are selected in this work: (1) 2,3-naphthalenedicarboxylic acid (H_2**ndc**)—an analogic but bulky derivative of 1,2-benzenedicarboxylic acid (H_2**bdc**) (see Chart 1) with an extended π-conjugated system—as the primary ligand, taking advantage of its versatile coordination ability and the steric bulk; (2) two 4,4′-bipyridyl-like bridging spacers with different extended lengths of the molecular backbones—namely, 4,4′-bipyridine (4bpy) and *trans*-4,4′-azobis(pyridine) (abp)—as reliable linkers for the construction of higher-dimensional coordination networks. Here, we report the syntheses and structural regulation, as well as luminescent and thermal properties of six Ag(I) and Zn(II) complexes with these ligands.

Experimental section

Materials and general methods

With the exception of the ligand abp that was prepared according to the literature procedure,[17] all the starting reagents and solvents for synthesis and analysis were commercially available and used as received. Elemental analyses were performed on a Vario EL III Elementar analyzer. IR spectra were recorded in 4000–400 cm^{-1} on a Tensor 27 OPUS (Bruker) FT-IR spectrometer with KBr pellets. Thermogravimetric (TG) analysis experiments were carried out on a Perkin–Elmer Diamond SII thermal analyzer from room temperature to 800 °C under N_2 atmosphere at a heating rate of 10 °C min^{-1}. The emission and excitation spectra of the solid samples were recorded on an F-7000 (Hitachi) spectrophotometer at room temperature.

Synthesis of complexes 1–6

[Ag_2(ndc)]$_\infty$ (1). A CH_3OH solution (15 mL) of $AgClO_4·6H_2O$ (0.1 mmol) was carefully layered on top of a water solution (10 mL) of H_2**ndc** (0.05 mmol) in the presence of NaOH (0.1 mmol for adjusting the pH value) in a test tube. Yellowy prism single crystals suitable for X-ray analysis appeared at the tube wall after *ca.* one month at room temperature. Yield: ~40% (based on H_2**ndc**). Calcd. (found) for $C_{12}H_6Ag_2O_4$ (429.91): C, 33.53 (33.68); H, 1.41 (1.34)%. IR (cm^{-1}): 3422 (m, br), 3051 (m), 2128 (w), 1929 (w), 1815 (w), 1632 (m), 1559 (vs), 1508 (s), 1460 (s), 1398 (vs), 1315 (m), 1274 (w), 1206 (w), 1141 (m), 1042 (w), 954 (w), 898 (m), 854 (m), 813 (m), 777 (m), 749 (m), 695 (w), 647 (w), 603 (m), 584 (m), 543 (w), 507 (w), 479 (m), 421 (w).

{[Zn(ndc)(H_2O)](H_2O)}$_\infty$ (2). A solution of $Zn(ClO_4)_2·6H_2O$ (0.1 mmol) in CH_3OH (10 mL) was added to H_2**ndc** (0.05 mmol) in the presence of 2,6-dimethylpyridine (*ca.* 0.05 mL for adjusting the pH value) with stirring for *ca.* 30 min. The resulting white solid was filtered off and the solution was kept at room temperature. Colorless single crystals suitable for X-ray analysis were obtained

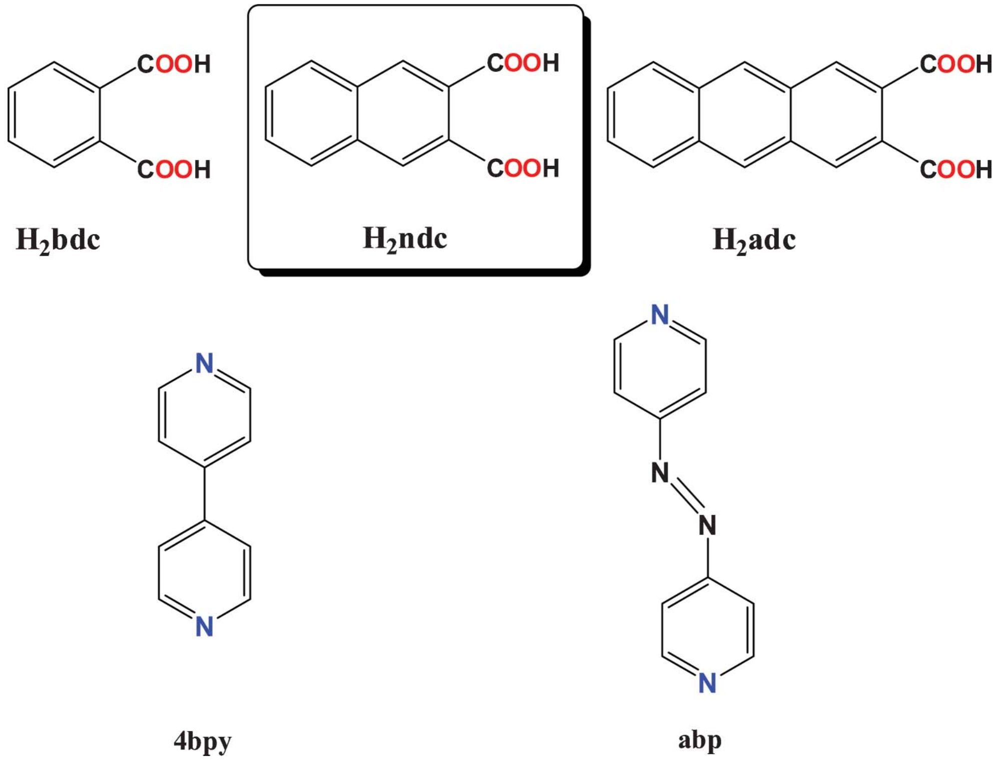

Chart 1

by slow evaporation of the solvent after *ca.* two weeks. Yield: ~30% (based on H_2**ndc**). Calcd. (found) for $C_{12}H_{10}O_6Zn$ (315.57): C, 45.67 (45.79), H, 3.19 (3.34)%. IR (cm^{-1}): 3219 (s, br), 1539 (s), 1481 (m), 1453 (m), 1408 (s), 1237 (w), 1212 (w), 1145 (w), 1050 (w), 964 (w), 902 (w), 880 (w), 828 (m), 808 (m), 760 (m), 696 (w), 652 (s), 620 (m), 600 (w), 476 (m), 430 (w).

$\{[Ag_2(ndc)(4bpy)_2][Ag(4bpy)(H_2O)](ClO_4)(H_2O)_2\}_\infty$ (3). An ammonia solution ($NH_3 \cdot H_2O$, 0.01 M for adjusting the pH value) was dropped slowly into a solution of $AgClO_4 \cdot 6H_2O$ (0.05 mmol) in CH_3OH–H_2O (5 mL, v/v = 3 : 2) with stirring for *ca.* 15 min. With that, H_2**ndc** (0.05 mmol) and 4bpy (0.05 mmol) were in turn added to the above solution and stirred for *ca.* 30 min. The resulting white suspension was filtered off and the filtrate was kept at room temperature. Colorless single crystals suitable for X-ray analysis were obtained by slow evaporation of the solvent after *ca.* one week. Yield: ~40% (based on H_2**ndc**). Calcd. (found) for $C_{42}H_{36}Ag_3ClN_6O_{11}$ (1159.83): C, 43.49 (43.58), H, 3.13 (3.24), N, 7.25 (7.36)%. IR (cm^{-1}): 3420 (s, br), 3049 (w), 2971 (w), 2355 (w), 1940 (w), 1842 (w), 1598 (vs), 1565 (vs), 1487 (m), 1447 (m), 1411 (s), 1382 (m), 1317 (m), 1262 (w), 1220 (m), 1184 (w), 1095 (s), 961 (w), 935 (w), 885 (w), 807 (s), 781 (w), 709 (w), 684 (w), 659 (w), 627 (m), 582 (w), 535 (m), 485 (w).

$[Zn_5(ndc)_4(4bpy)_2(\mu_3\text{-}OH)_2]_\infty$ (4). A mixture of H_2**ndc** (0.05 mmol) and 4bpy (0.05 mmol) in CH_3OH (10 mL) in the presence of 2,6-dimethylpyridine (0.05 mL for adjusting the pH value) was carefully layered onto a water solution (15 mL) of $Zn(ClO_4)_2 \cdot 6H_2O$ (0.1 mmol) in a test tube. Colorless single crystals suitable for X-ray analysis were observed at the tube wall after *ca.* three weeks. Yield: ~40% (based on H_2**ndc**). Calcd. (found) for $C_{68}H_{42}N_4O_{18}Zn_5$ (1529.91): C, 53.38 (53.29), H, 2.77 (2.92), N, 3.66 (3.81)%. IR (cm^{-1}): 3462 (s, br), 3055 (m), 1605 (s), 1466 (s), 1407 (s), 1223 (m), 1142 (m), 1066 (m), 1009 (w), 954 (w), 900 (m), 870 (m), 806 (s), 763 (m), 654 (m), 621 (m), 592 (m), 545 (w), 460 (m), 422 (m).

$\{[Ag(ndc)(abp)][Ag(abp)](H_2O)_3\}_\infty$ (5). The same procedure as that for **1** was used except for the introduction of auxiliary co-ligand abp (0.05 mmol). Yellowy block single crystals suitable for X-ray analysis appeared at the tube wall after *ca.* two weeks at room temperature. Yield: ~50% based on H_2**ndc**. Calcd. (found) for $C_{32}H_{28}Ag_2N_8O_7$ (852.36): C, 45.09 (45.17), H, 3.31 (3.24), N, 13.15 (13.36)%. IR (cm^{-1}): 3422 (m, br), 3092 (m), 2242 (w), 1598 (s), 1566 (vs), 1447 (w), 1413 (s), 1381 (s), 1348 (s), 1245 (w), 1221 (m), 1141 (w), 1107 (w), 1047 (w), 965 (w), 921 (w), 897 (w), 846 (m), 817 (w), 794 (w), 771 (m), 663 (w), 602 (w), 568 (m), 526 (w), 481 (w), 439 (w).

$\{[Zn_2(ndc)_2(abp)(H_2O)_2](H_2O)_2\}_\infty$ (6). The same procedure as that for **4** was used except for the use of abp (0.05 mmol) instead of 4bpy. Claret-red single crystals were obtained in ~30% yield (based on H_2**ndc**). Calcd. (found) for $C_{17}H_{14}N_2O_6Zn$ (407.67): C, 50.08 (50.21), H, 3.46 (3.61), N, 6.87 (7.01)%. IR (cm^{-1}): 3438 (s, br), 2973 (m), 2355 (w), 1810 (w), 1608 (s), 1571 (s), 1469 (m), 1448 (m), 1370 (s), 1225 (m), 1141 (w), 1090 (w), 1047 (m), 910 (w), 850 (m), 811 (m), 776 (m), 753 (w), 683 (w), 600 (w), 570 (w), 480 (w).

Caution! Although we have met no problem in handling the metal perchlorates during this work, they should be treated cautiously due to their potentially explosive nature.

X-Ray powder diffraction

X-Ray powder diffraction patterns (PXRD) of **1–6** were recorded at room temperature on a Bruker D8 Advance diffractometer (Cu-Kα, λ = 1.54056 Å) operated at 40 kV and 30 mA, using a Cu-target tube and a graphite monochromator. The crushed single-crystalline powder samples were prepared by crushing the crystals and the intensity data were recorded by continuous scan in a $2\theta/\theta$ mode from 3° to 80°, with a step size of 0.02° and a scan speed of 8° min^{-1}. Simulation of PXRD patterns was carried out by using the single-crystal data and diffraction-crystal module of the *Mercury* program.

Crystal structure determination

X-Ray single-crystal diffraction data for **1–6** were collected on a Bruker Smart 1000 CCD area-detector diffractometer at 294(2) K with Mo-Kα radiation (λ = 0.71073 Å) by ω scan mode. The program SAINT[18] was used for integration of the diffraction profiles and a semi-empirical absorption correction was applied using the SADABS program.[19] All of the structures were solved by direct methods using the SHELXS program of the SHELXTL package and refined by full-matrix least-squares methods with SHELXL.[20] Metal ions in all the complexes were located from the *E*-maps, and the other non-H atoms were located in successive difference Fourier syntheses and refined with anisotropic thermal parameters on F^2. Hydrogen atoms except for those of water were generated theoretically and refined with isotropic thermal parameters riding on the parent atoms. Crystallographic data and structural refinement details for **1–6** are summarized in Table 1. Hydrogen-bonding geometries for complexes **3**, **5**, and **6** are listed in Table 2.

Results and discussion

Synthetic consideration and general characterization

For a systematic study of the Ag(I) and Zn(II) coordination polymers with **ndc**, our strategy was to change the metal centers or 4,4′-bipyridyl-like bridging co-ligands with different *N*,*N*′-donor separations of the molecular backbones (*ca.* 7 Å for 4bpy and *ca.* 9 Å for abp) in the reaction systems. When a direct combination of the Ag(I) or Zn(II) salt and organic ligands was employed, using the conventional solution method followed by solvent evaporation, single crystals suitable for X-ray diffraction could be readily obtained for **2** and **3**. However, similar attempts were not successful for the synthesis of complexes **1** and **4–6**, either providing no evidence of solid formation or resulting in a mass of uncharacterized microcrystalline solids. In general, properly lowering the reaction rate may facilitate the growth of well-shaped single crystals,[21a] and considering this, the isolation of **1** and **4–6** were carried out by using the diffusion method.

IR spectra of **1–6** show features attributable to the compositions of the complexes.[21b] The broad bands centered at *ca.* 3219–3462 cm^{-1} (3422 cm^{-1} for **1**, 3219 cm^{-1} for **2**, 3420 cm^{-1} for **3**, 3462 cm^{-1} for **4**, 3422 cm^{-1} for **5**, and 3438 cm^{-1} for **6**) indicate the O–H stretching of hydroxyl or water.[12,22] For **1–6**, the characteristic bands of carboxylate groups appear in the region at 1608–1508 cm^{-1} for the antisymmetric stretching vibrations and at 1466–1370 cm^{-1} for the symmetric stretching vibrations. Furthermore,

Table 1 Crystallographic data and structure refinement summary for complexes **1–6**

	1	**2**	**3**	**4**	**5**	**6**
Empirical formula	$C_{12}H_6Ag_2O_4$	$C_{12}H_{10}O_6Zn$	$C_{42}H_{36}Ag_3ClN_6O_{11}$	$C_{68}H_{42}N_4O_{18}Zn_5$	$C_{32}H_{28}Ag_2N_8O_7$	$C_{17}H_{14}N_2O_6Zn$
Formula weight	429.91	315.57	1159.83	1529.91	852.36	407.67
Crystal system	Monoclinic	Orthorhombic	Monoclinic	Triclinic	Triclinic	Orthorhombic
Space group	$P2_1/c$	$Pbca$	$P2_1/c$	$P\bar{1}$	$P\bar{1}$	$Aba2$
a/Å	17.195(4)	10.8248(5)	10.9218(4)	7.2752(7)	9.8037(6)	22.2072(7)
b/Å	6.2492(7)	8.8552(4)	17.1519(5)	13.8489(15)	12.9170 (7)	13.0160(5)
c/Å	10.7732(14)	25.3482(13)	22.5719(6)	15.5737(14)	13.5314	11.4239(7)
α (°)	90	90	90	84.229(8)	87.233(4)	90
β (°)	100.507(16)	90	99.906(3)	88.532(7)	79.209(5)	90
γ (°)	90	90	90	84.578(8)	70.022(5)	90
V/Å^3	1138.2(3)	2429.8(2)	4165.3(2)	1554.0(3)	1581.72(15)	3302.1(3)
Z	4	8	4	1	2	8
D/g cm^{-3}	2.509	1.725	1.849	1.635	1.790	1.640
μ/mm^{-1}	3.441	2.041	1.531	1.980	1.301	1.526
R_{int}	0.0472	0.0534	0.0593	0.0484	0.0261	0.0383
GOF	1.048	1.051	0.985	1.061	1.070	1.001
$R_1{}^a/wR_2{}^b$ [$I > 2\sigma(I)$]	0.0419/0.0774	0.0279/0.0473	0.0372/0.0480	0.0456/0.0840	0.0324/0.0373	0.0325/0.672
ρ_{max}/ρ_{min}/e Å^{-3}	2.033/−0.744	0.241/−0.382	0.607/−0.513	1.093/−0.487	0.836/−0.456	0.409/−0.236

^{a} $R_1 = \Sigma(\|F_o| - |F_c\|)/\Sigma|F_o|$; ^{b} $wR_2 = [\Sigma w(|F_o|^2 - |F_c|^2)^2/\Sigma w(F_o{}^2)^2]^{1/2}$.

Table 2 Hydrogen-bonding geometry (Å, °) for **3**, **5**, and **6**

D–H···A	d(D–H)	d(H···A)	d(D···A)	∠D–H···A
3				
O9–H91···O4	0.850	2.09	2.633(5)	121
O9–H92···O10^a	0.850	1.97	2.698(6)	143
O10–H2W···O1^b	0.850	1.98	2.791(6)	159
C33–H33A···$Cg1^c$	0.930	3.18	3.751(5)	122
C33–H33A···$Cg2^c$	0.930	3.07	3.980(5)	168
C34–H34A···$Cg1^c$	0.930	2.86	3.575(5)	135
C25–H25A···O4^d	0.930	2.27	3.125(6)	153
C39–H39A···O4^a	0.930	2.59	3.405(6)	146
5				
C2–H2A···O2^a	0.930	2.46	3.224(9)	140
O6–H3W···O4^b	0.850	1.88	2.731(7)	174
O6–H4W···O4^c	0.850	1.90	2.742(1)	171
6				
OIW–H1WB···O3^a	0.850	2.12	2.839(5)	142

Symmetry codes for **3** ($Cg1$ and $Cg2$ are the centroids of C2–C4/C9–C11 and C4–C9 rings in **ndc** ligands, respectively): a = $-x, -y, -z + 2$; b = $-x - 1, -y, -z + 2$; c = $-x - 1, y - 1/2, -z + 3/2$; d = $-x, y + 1/2, -z + 5/2$; for **5**: a = $-x, -y + 1, -z + 1$; b = $x + 1, y, z - 1$; c = $-x, y - 2, -z + 1$; for **6**: a = $-x + 3/2, y, z + 1/2$.

the $\Delta\nu$ [$\nu_{as}(COO^-) - \nu_s(COO^-)$] values indicating the coordination modes of carboxylate in **ndc** (see Scheme 1) are 48, 99, 110, and 161 cm^{-1} for **1**, 131 cm^{-1} for **2**, 154 and 187 cm^{-1} for **3**, 139 and 198 cm^{-1} for **4**, 185 cm^{-1} for **5**, and 201 and 238 cm^{-1} for **6**, respectively, which are consistent with their solid structural features.[12,22]

Description of the crystal structures for 1–6

[Ag$_2$(ndc)]$_\infty$ (1). Single crystal X-ray diffraction analysis of **1** indicates a 2-D layered coordination network. The asymmetric unit contains two Ag(I) ions and one fully deprotonated **ndc** ligand (Fig. 1a). Both Ag1 and Ag2 centers are four-coordinated by four O$_{carboxylate}$ atoms from different **ndc** ligands with a distorted tetrahedral geometry (Ag1–O: 2.222(5)–2.593(5) Å; Ag2–O: 2.286(5)–2.409(6) Å; O–Ag1–O: 80.7(2)–156.74(18)°; O–Ag2–O: 91.68(18)–131.45(11)°; see Table S1 for detailed bond parameters, ESI†). All Ag–O bond parameters are in the normal range expected for similar complexes in the literature.[6,11c,12e,23,24] Also, a short Ag···Ag interaction (2.9502(9) Å) is observed between Ag1 and Ag2 bridged by carboxylate, which is similar to those found in other complexes with Ag···Ag contacts (the Van der Waals Ag···Ag contact distance being 3.40 Å), and slightly longer than that found in metallic silver (2.889 Å).[25] It is worthwhile to note that each **ndc** ligand coordinates to eight Ag(I) center (four Ag1 and four Ag2), in which the carboxylate groups adopt the different μ_5-η^3:η^2-*syn*, *syn*/*syn*, *trans* mode for O1–C1–O2 and μ_3-η^2:η^1-*syn*, *syn*/*syn*, *trans* fashion for O3–C12–O4 (see Scheme 1a and Fig. S1, ESI†). To the best of our knowledge, the former μ_5-bridging mode has not been reported in metal-dicarboxylate coordination polymers so far. As a result, a novel sandwich-like 2-D coordination network is constructed, running parallel to the (100) plane, with two naphthalene-ring walls in both sides and one in-between the Ag–O$_{carboxylate}$ sheet (see Fig. 1b).

A better insight into the complicated 2-D motif of **1** can be achieved by using the topological approach.[26] If neglecting the Ag1···Ag2 interactions, each **ndc** ligand is linked to four Ag1

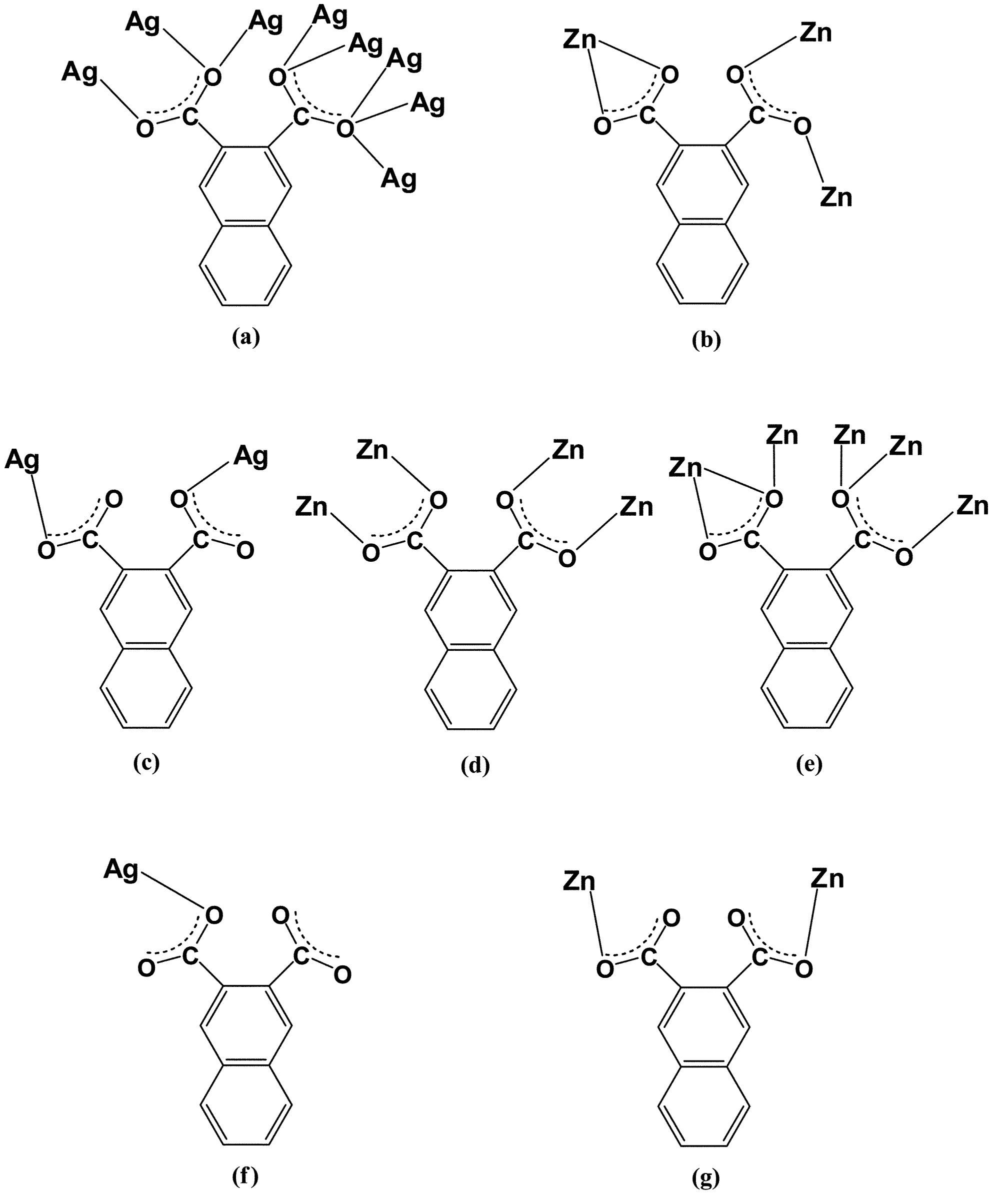

Scheme 1 Coordination modes for **ndc** in **1–6**.

and four Ag2 and thus, can be regarded as a non-planar 8-connecting node. Both Ag1 and Ag2 are connected to four distinct **ndc** ligands, respectively, acting as tetrahedral 4-connected nodes. The resulting (4,8)-connected 2-D topological net (see Fig. S2, ESI†) has an overall Schläfli symbol of $(4^6)_2(4^{16}.6^{11}.8)$. On the other hand, if one further considers the Ag1 ··· Ag2 bimetallic unit as a non-planar 5-connected node (see Fig. 1c) that is linked to five **ndc** ligands, and each **ndc** ligand as a square-pyramidal 5-connected node under this condition. Such a 2-D network exhibits a very rare example for 5-connected topology with the Schläfli symbol of $(4^8.6^2)$, instead of the known 5-connecting patterns with trigonal-bipyramidal or square-pyramidal nodes, such as **bnn** net (or boron nitride) $(4^6.6^4)$,[27a] **sqp** net $(4^4.6^6)$,[27b] **nov** net $(4^4.6^6)$,[27c,d] and 6^{10}-nets (**1oh**,[27e] **ghw**,[27f] **rld-z**,[27g] and **fnu**[27h]). Networks with 5-connectivity are quite limited, owing to the difficulty in generating 5-connecting metal centers/clusters and organic tectons.[26] Thus far, only several examples for 5-connected coordination polymers have been reported.[27,28] Compared with the simplest 5-connected nets **bnn** $(4^6.6^4)$ and **sqp** $(4^4.6^6)$ based on regular trigonal-bipyramidal and square-pyramidal nodes, the 5-connected $(4^8.6^2)$ net of **1** contains two types of equivalent nodes (see Fig. 1c) with the long vertex symbol of $(4.4.4.4.4.4.4.4.6_3.6_3)$ for both **ndc** ligands and Ag1–Ag2 bimetallic units, which result in the non-planar feature of the 2-D motif. A careful examination of the RCSR, EPINET, and TOPOS databases[29] indicates that this topological net is unprecedented.

$\{[Zn(ndc)(H_2O)](H_2O)\}_\infty$ (2). Single crystal X-ray diffraction analysis reveals a 2-D layered coordination structure of **2**. The asymmetric unit is composed of one Zn(II) ion, one **ndc** ligand, one water ligand, and one lattice water molecule (Fig. 2a). Each Zn(II) ion is five-coordinated to four carboxylate O atoms from three different **ndc** ligands and one water ligand. The geometry around Zn(II) can be best described as a distorted square pyramid. The

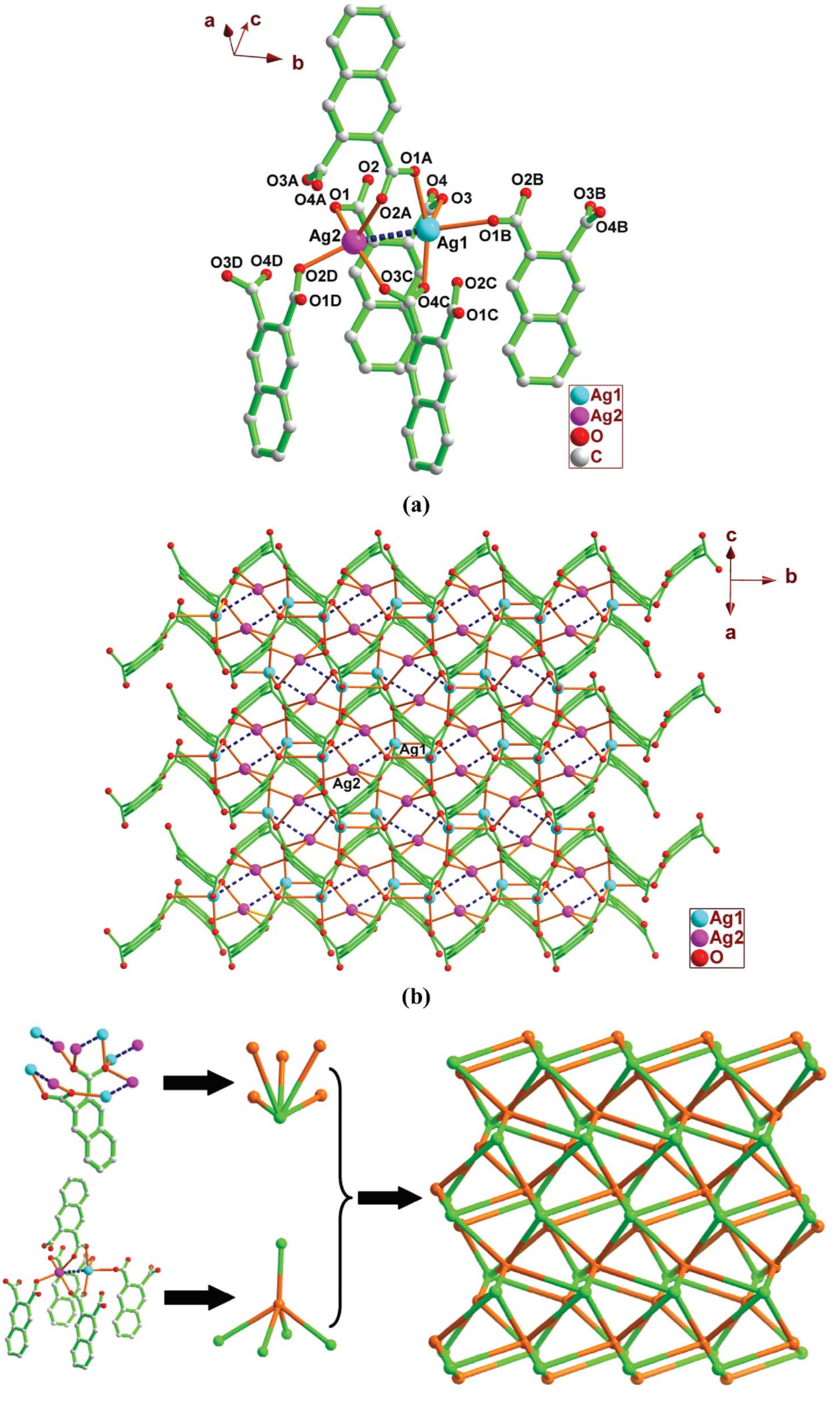

(a)

(b)

(c)

Fig. 1 Views of **1**. (a) Coordination environment of Ag(I) showing the Ag1 ··· Ag2 interactions (blue dashed lines) (A = −x + 1, −y + 2, −z + 1; B = x, y − 1, z; C = x, −y + 3/2, z + 1/2; D = x, −y + 5/2, z + 1/2). (b) 2-D layer running parallel to the (100) plane. (c) A schematic representation of the 2-D 5-connected network with the Schläfli symbol of ($4^8.6^2$), illustrating the connectivity of Ag1 ··· Ag2 units (orange spheres) and **ndc** ligands (green spheres).

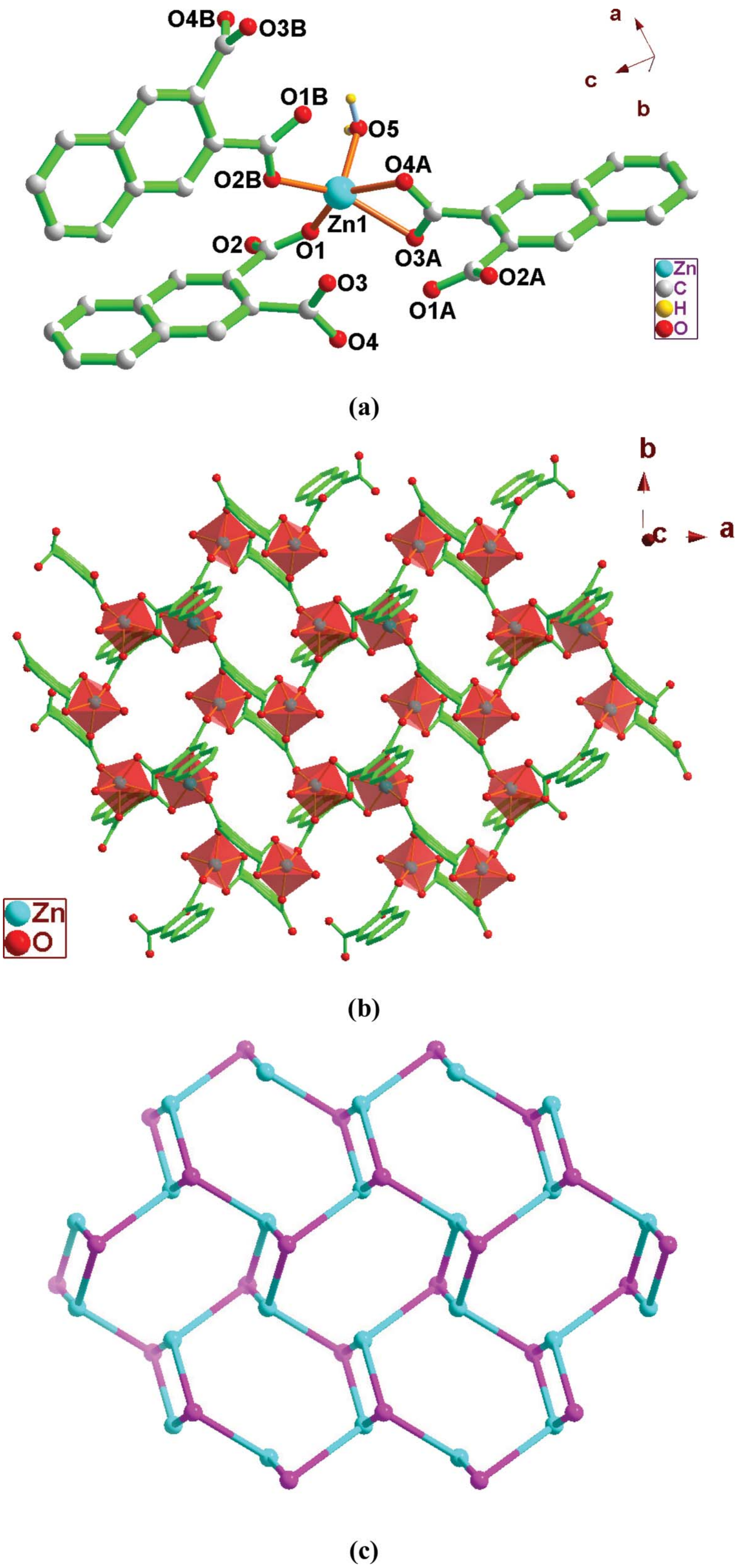

Fig. 2 Views of **2**. (a) Coordination environment of Zn(II) (A = −*x*, −*y*, −*z* + 1; B = −*x* + 1/2, *y* − 1/2, *z*). (b) 2-D layer viewed along the *c* axis. (c) A schematic representation of the 2-D (4.8^2) topology (cyan spheres for Zn(II) and pink spheres for **ndc**).

Zn–O bond distances lie in the range of 1.959(2)–2.230(2) Å with the bond angles around Zn(II) ranging from 59.46(7) to 153.58(9)° (see Table S2 for detailed bond parameters, ESI†). Moreover, the carboxylate groups of **ndc** adopt the chelating and *syn-anti* bridging coordination modes (Scheme 1b and Fig. S3, ESI†). From the viewpoint of topology, both Zn1 and **ndc** can be regarded as the 3-connected nodes, and the resulting 2-D layer has a (4.8^2) topology (see Fig. 2b and 2c).

{[Ag$_2$(ndc)(4bpy)$_2$][Ag(4bpy)(H$_2$O)](ClO$_4$)(H$_2$O)$_2$}$_\infty$ (3). When the linear spacer 4bpy was introduced to the assembled system, a novel 1-D complex **3** was produced. This structure consists of two almost parallel 1-D motifs running along the [001] direction, that is, a neutral double-chain $[Ag_2(\mathbf{ndc})(4bpy)_2]_\infty$ (denoted as chain **A**) and a cationic single chain $[Ag(4bpy)(H_2O)]_\infty$ (denoted as chain **B**) (see Fig. 3). The asymmetric unit contains three Ag(I) centers, one fully deprotonated **ndc** ligand, three 4bpy ligands, one water ligand, one free perchlorate, and two lattice water molecules. In chain **A**, there are two different Ag(I) centers (Ag1 and Ag2), in which the Ag···Ag separations across the **ndc** and 4bpy ligands are 3.4468(6) and 11.3295(7) Å. Both Ag1 and Ag2 are 3-coordinated, adopting a slightly distorted T-shaped geometry that is surrounded by two pyridyl N donors from different 4bpy and one carboxylate O from **ndc** (Ag1–O1: 2.582(3) Å; Ag2–O3: 2.547(3) Å; Ag1–N1/N2: 2.140(4)–2.147(4) Å; Ag2–N1/N2: 2.128(4)–2.138(4) Å; N–Ag1–N/O: 92.48(14)–164.78(15)°; N–Ag2–N/O: 82.22(13)–169.34(16)°; see Table S3, ESI†). In chain **B**, the Ag3 center also takes a T-shaped geometry, provided by two pyridyl N atoms from two 4bpy and one water ligand with the closest intrachain Ag···Ag separation of 11.4770(7) Å. Both carboxylate groups of the **ndc** ligand adopt the monodentate binding mode (see Scheme 1c and Fig. S4, ESI†). Two adjacent chains **A** and **B** are further linked by interchain π···π interactions between the pyridyl rings of 4bpy (centroid–centroid distances: 3.738–3.740 Å, interplanar distances: 3.5269–3.5888 Å, dihedral angles: 1.1–4.9°),[30] O–H···O H-bonds (O9–H91···O4, see Table 2) between the water ligand and **ndc**, and weak Ag3···O4 (2.6693(3) Å) contacts, which thus afford an overall 1-D **A** + **B** pattern along the *c* axis (see Fig. 3).

In addition, the adjacent 1-D **A** + **B** motifs aforementioned are further assembled into two types of perpendicular 2-D sheets along (010) and (100), respectively (see Figs. S5 and S6, ESI†), by interchain O–H···O H-bonds (O9–H92···O10 and O10–H2W···O1, see Table 2) between the lattice water molecules and chains **A** and **B**, C–H···O interactions[31] (C25–H25A···O4 and C39–H39A···O4; see Table 2) between **ndc** and 4bpy, and C–H···π interactions[32] (d = 2.860, 3.066, and 3.175 Å; A = 134, 168, and 122°; d and A stand for H···π separation and C–H···π angle in the C–H···π pattern, see Table 2) between the naphthyl and/or pyridyl groups of **ndc** and 4bpy with an edge-to-face orientation, as calculated by PLATON,[33] which further construct a 3-D supramolecular framework.

[Zn$_5$(ndc)$_4$(4bpy)$_2$(μ$_3$-OH)$_2$]$_\infty$ (4). When the bridging co-ligand 4bpy was introduced to the reaction system of **2**, a 3-D coordination framework **4** was obtained, in which three kinds of Zn(II) ions are linked by carboxylate and hydroxyl groups to constitute a trinuclear unit (see Fig. 4a). Zn1 lies on an inversion center with an octahedral geometry, provided by two μ_3-OH$^-$ groups (Zn1–O9 = 2.039(3) Å) and four carboxylate O donors from four **ndc** ligands (Zn–O: 2.054(4)–2.196(3) Å). Zn2 is coordinated by four carboxylate O atoms (Zn–O: 2.027(4)–2.216(4) Å) from three **ndc** ligands, one μ_3-OH$^-$ ion (Zn2–O9 = 2.114(3) Å), and one N donor from 4bpy (Zn2–N1: 2.231(4) Å) to show a distorted octahedral sphere. Zn3 also has an approximately octahedral geometry, which is ligated by one N donor from 4bpy (Zn3–N2: 2.129(4) Å), four carboxylate O atoms from three **ndc** ligands (Zn–O: 2.074(4)–2.369(4) Å), and one μ_3-OH$^-$ (Zn3–O9 = 2.042(3) Å). It should be noted that the μ_3-OH$^-$ group is not co-planar with Zn1–Zn2–Zn3, with a deviation of *ca.* 0.64 Å. All Zn–O distances are comparable to those found in the literature (see Table S4, ESI†).[12] Three kinds of binding modes of carboxylate groups are found, namely, μ_2-η^1:η^1-*syn-syn* bridging, μ_2-η^1:η^2-bridging/chelating, and μ_3-η^1:η^2-bridging modes (Scheme 1d,e and Fig. S7, ESI†).

The Zn(II) ions are connected by the **ndc** ligands to produce a 1-D array along the *a*-axis (see Fig. 4b, left). Furthermore, these 1-D motifs are interconnected by the 4bpy bridges to afford a complicated 3-D framework (Fig. 4b, right). From the view of topology, the **ndc** ligand adopts the 4-connected mode to link four Zn(II) ions. Zn1 and Zn2/Zn3 can be regarded as the 6- and 5-connected nodes, respectively. In addition, the hydroxyl ion takes the 3-connected mode to link three Zn(II) ions (Zn1, Zn2, and Zn3). Thus, the resulting multi-connected network (see Fig. 4c) has the Schläfli symbol of $(4^3)(4^3.6^3)(4^3.6^5.8^2)(4^4.6^4.8^2)(4^{10}.6^5)$ (representing hydroxyl/**ndc**/Zn3/Zn2/Zn1 nodes, respectively).[26]

{[Ag(ndc)(abp)][Ag(abp)](H$_2$O)$_3$}$_\infty$ (5). To further explore the effect of relevant 4,4′-bipyridyl-like spacers on Ag–**ndc** coordination networks, an extended dipyridyl ligand abp was used to construct another 1-D coordination polymer **5**. This structure

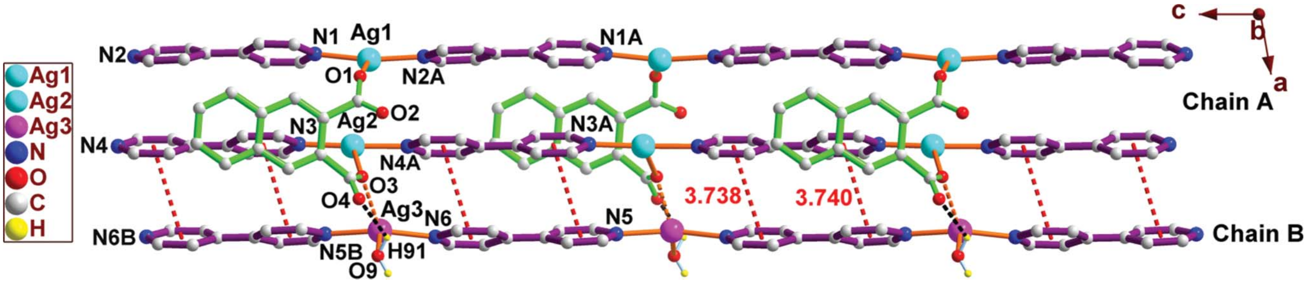

Fig. 3 View of the different 1-D chains **A** and **B** along [001] in **3**, showing the coordination environments of Ag1 and Ag2 (cyan spheres) in chain **A** and Ag3 (pink spheres) in chain **B** as well as interchain π···π stacking (red dashed lines), O–H···O hydrogen-bonding (black dashed lines), and Ag3···O3 (orange dashed lines) interactions (A = x, $-y + 1/2$, $z - 1/2$; B = x, $-y + 1/2$, $z + 1/2$).

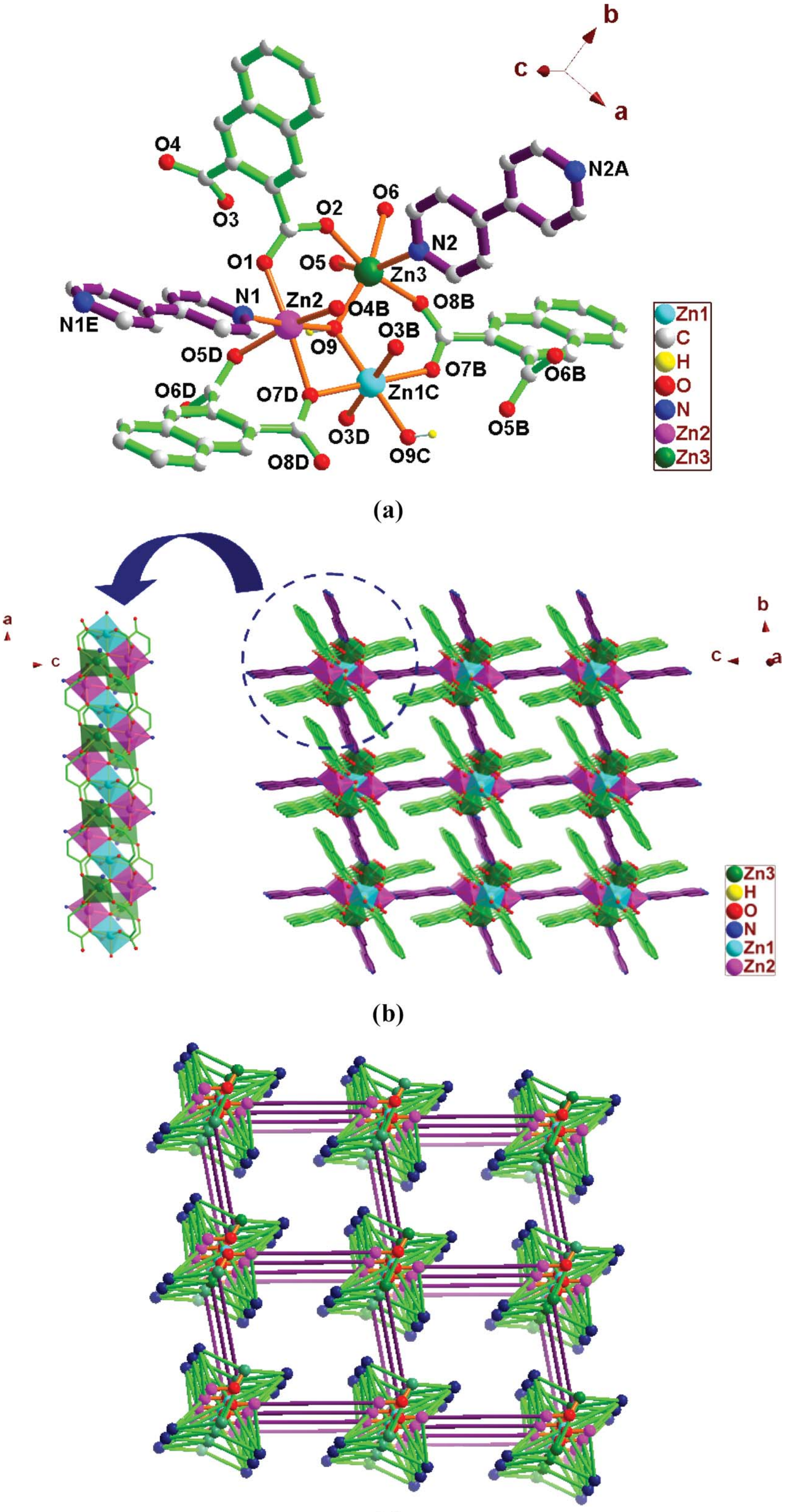

(a)

(b)

(c)

Fig. 4 Views of **4**. (a) Coordination environment of Zn(II) (A = $-x-1$, $-y+1$, $-z$; B = $x-1$, y, z; C = $-x-1$, $-y+2$, $-z$; D = $-x$, $-y+2$, $-z$; E = $-x$, $-y+2$, $-z-1$). (b) 3-D network viewed along the *a* axis, in which a 1D segment is extracted and highlighted (left). (c) A schematic representation of the (3,4,5,6)-connected net (cyan spheres: Zn1; pink spheres: Zn2; green spheres: Zn3; blue spheres: **ndc**; red spheres: hydroxyl; purple rods: 4bpy).

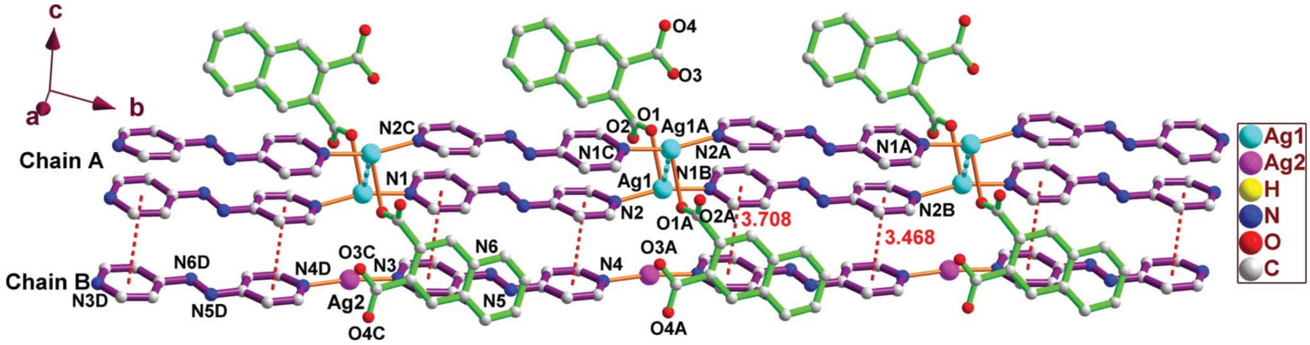

Fig. 5 View of the different 1-D chains **A** and **B** along [110] in **5**, showing the coordination environments of Ag1 (cyan spheres) in chain **A** and Ag2 (pink spheres) in chain **B** as well as interchain π···π stacking (red dashed lines) and Ag1···Ag1A (cyan dashed lines) interactions (A = −*x*, −*y* + 2, −*z* + 1; B = *x* − 1, *y* + 1, *z*; C = −*x* + 1, −*y* + 1 −*z* + 1; D = *x* + 1, *y* − 1, *z*).

(see Fig. 5) consists of two almost parallel 1-D coordination motifs running along the [110] direction, namely, a 1-D anionic chain $[Ag(\mathbf{ndc})(abp)]_\infty$ (denoted as chain **A**) and a 1-D cationic array $[Ag(abp)]_\infty$ (denoted as chain **B**). The fundamental building unit contains two Ag(I) ions (Ag1 and Ag2), one fully deprotonated **ndc** ligand, two abp ligands, and three lattice water molecules. In chain **A**, Ag1 adopts a distorted T-shaped sphere provided by two N donors of two abp ligands and one O atom of **ndc** (Ag1–O1: 2.552(3) Å; Ag1–N1/2: 2.177(2)–2.197(3) Å; N–Ag1–N/O: 90.76(9)–164.79(11)°, see Table S5, ESI†), with the centrosymmetric Ag1···Ag1A separation of 3.3607(7) Å. In chain **B**, the linear geometry of Ag2 is completed by two N donors from two abp ligands (Ag2–N3/N4: 2.163(2)–2.164(2) Å; N3–Ag2–N4: 173.13(13)°), with the adjacent Ag···Ag distance of 13.2827(1) Å. The **ndc** ligand in **3** takes the monodentate binding mode (see Scheme 1f and Fig. S8, ESI†) by using only one carboxylate (O1–C28–O2). Two adjacent chains **A** and **B** are linked by the interchain π···π stacking interactions between the pyridyl rings of abp (centroid-centroid distances: 3.468–3.708 Å, interplanar distances: 3.2474–3.4187 Å, dihedral angles: 3.4–5.2°), resulting in an overall 1-D **A** + **B** coordination array along the [110] direction (see Fig. 5).

Similar to that in **3**, the adjacent **A** + **B** motifs aforementioned are further assembled into two different 2-D sheets, running parallel to the (111) and (001) planes (see Figs. S9 and S10, ESI†) by interchain O–H···O H-bonds (O6–H3W···O4 and O6–H4W···O4, see Table 2 for details) between the lattice water molecules and chains **A** as well as C–H···O contacts between **ndc** and abp (C2–H2A···O2; see Table 2 for details),[31] which thus lead to the formation of a 3-D supramolecular framework (see Fig. S11, ESI†).

$\{[Zn_2(\mathbf{ndc})_2(abp)(H_2O)_2](H_2O)_2\}_\infty$ **(6).** The structure of **6** is a neutral 2-D network and the asymmetric unit is composed of one Zn(II) ion, one **ndc** ligand, half an abp ligand, one water ligand, and one lattice water molecule. Each Zn(II) center is four-coordinated by two carboxylate O atoms (Zn–O: 1.979(3)–2.038(3) Å) from different **ndc** ligands in monodentate mode (see Scheme 1g and Fig. S12, ESI†), one N-atom donor from abp (Zn–N: 2.064(3) Å), and one water ligand (Zn–O: 1.957(3) Å), showing a distorted tetrahedral geometry (see Fig. 6a and Table S6, ESI†). As a result, the Zn(II) ions are connected by **ndc** and abp bridges to result in a 2-D (6^3) topology network (see Fig. 6b and Fig. S13, ESI†).[26] In addition, the adjacent 2-D arrays are extended into a 3-D supramolecular framework (see Fig. S14, ESI†) *via* O1W–H1WB···O3 bonds (see Table 2 for details) and interlayer π···π stacking interactions between the pyridyl and naphthalene rings (centroid–centroid and interplanar separations: 3.664 and 3.534 Å; dihedral angle: 14.2°).[30]

Effect of the bulky naphthalene skeleton on structural assembly of 1–6

As typical aromatic carboxylic acid ligands, benzene-based dicarboxylic acids (especially $H_2\mathbf{bdc}$, see Chart 1) have been widely applied to construct Zn(II) and Ag(I) coordination frameworks.[5,6] However, the rational use of naphthalene-based dicarboxyl analogues, such as naphthalene-2,3-dicarboxylic acid ($H_2\mathbf{ndc}$, see Chart 1) with a larger π-conjugated system and the bulky aromatic skeleton, has been less documented so far.[16] From the above discussion of crystal structures, it can be seen that, in comparison with $H_2\mathbf{bdc}$, the $H_2\mathbf{ndc}$ ligand has two obvious characteristics: (1) the electronic nature of its extended π-conjugated system and the steric hindrance of the bulky naphthalene ring, which may affect not only the coordination fashion of carboxylate but also offer greater possibility for the formation of secondary interactions, and thus determine the final coordination arrays; (2) the extended π-conjugated system that normally results in C–H···π and/or π···π stacking interactions from the viewpoint of the electronic nature, along with the increased overlap of the aromatic surface areas, which will play an important role in forming the final supramolecular lattices, extending the low-dimensional coordination entities into higher-dimensional supramolecular networks. These characteristics cause $H_2\mathbf{ndc}$ to show different building functions compared with its benzene-based analogue $H_2\mathbf{bdc}$. As for the $H_2\mathbf{bdc}$ tecton, for instance, a mononuclear Zn(II) complex $[Zn(H\mathbf{bdc})_2(H_2O)_2]$[5i] as well as a dinuclear and a tetranuclear Ag(I) species, $[Ag_2(\mathbf{bdc})(NH_3)_2]$[6e] and $[Ag_4(\mathbf{bdc})_2(py)_6]$[6f] (py = pyridine) respectively, have been known. However, when we used $H_2\mathbf{ndc}$ instead of $H_2\mathbf{bdc}$ to react with Zn(II) and Ag(I), respectively, a 2-D 3-connected (4.8^2) coordination network $\{[Zn(\mathbf{ndc})(H_2O)](H_2O)\}_\infty$ (**2**) and an unusual 5-connected ($4^8.6^2$) layered motif $[Ag_2(\mathbf{ndc})]_\infty$ (**1**) were obtained. With regard to the coordination systems with mixed-ligands, we noticed that only a mononuclear complex $[Zn(H\mathbf{bdc})_2(4bpy)_2]$[5c] was reported. In contrast, when $H_2\mathbf{ndc}$ was used to react with Zn(II) or Ag(I) together with incorporating 4bpy

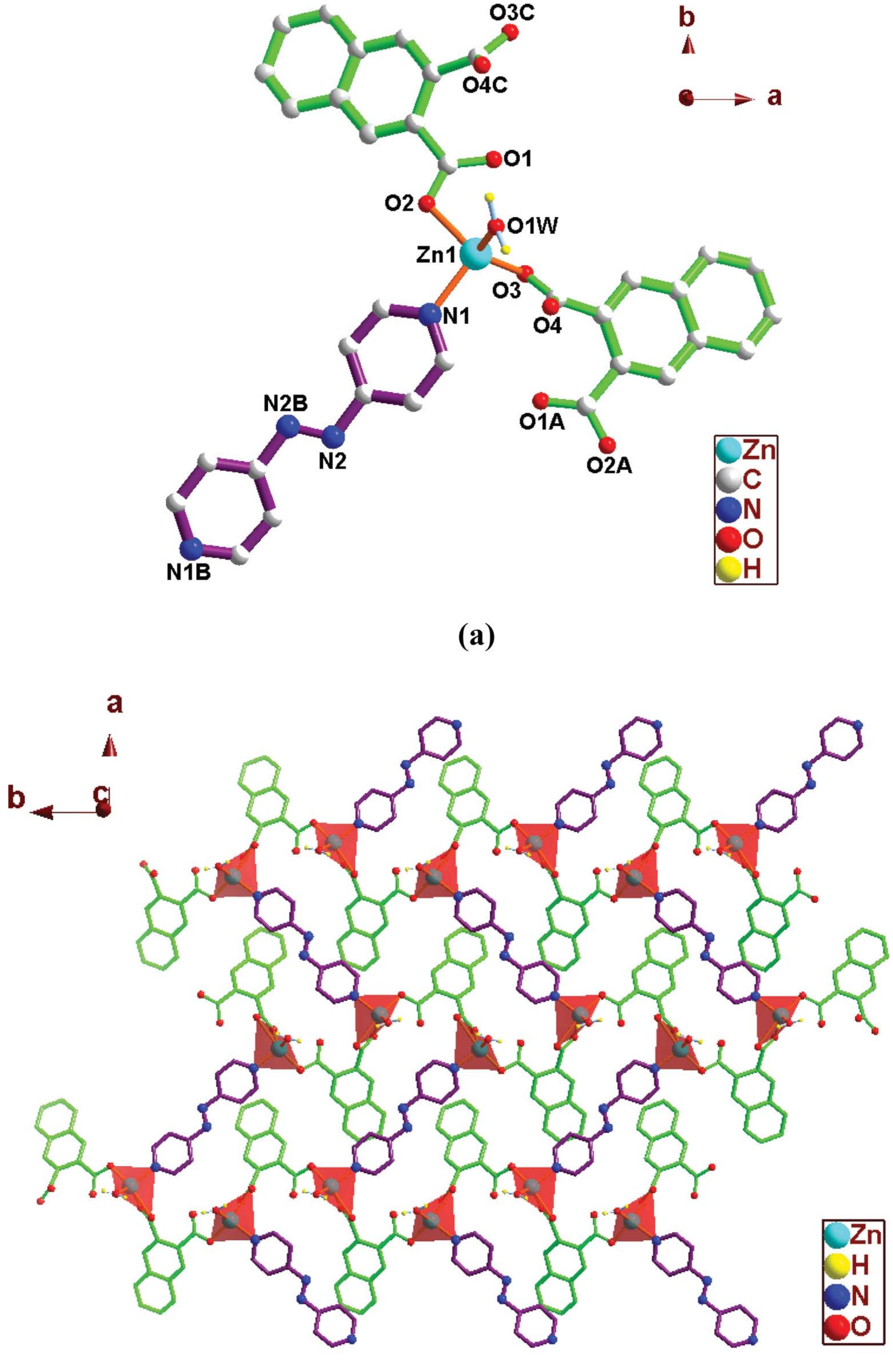

(a)

(b)

Fig. 6 Views of **6**. (a) Coordination environment of Zn(II) (A = $-x + 3/2, y - 1/2, z$; B = $-x + 1, -y + 1, z$). (b) 2-D layer viewed along the *c* axis.

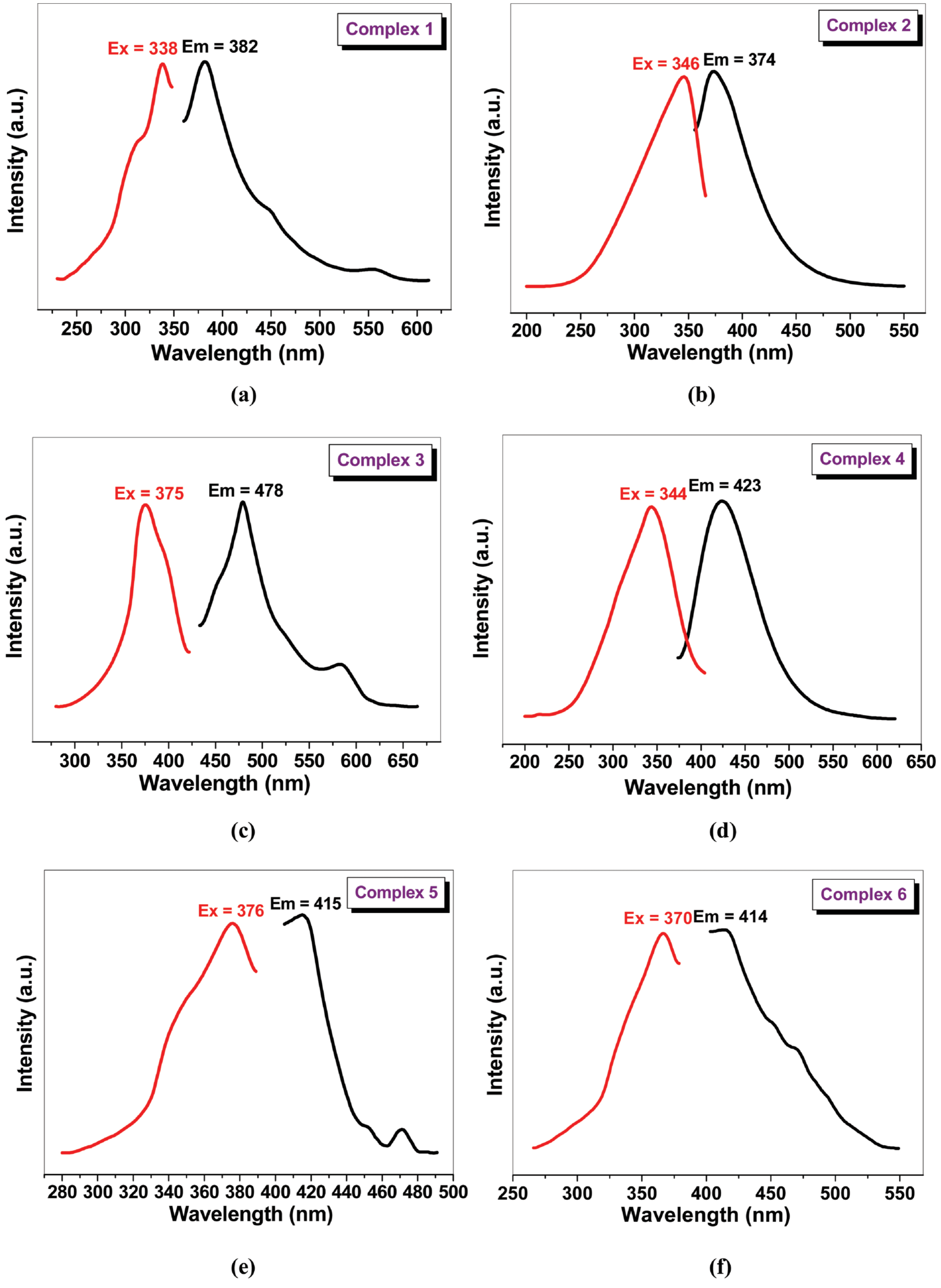

Fig. 7 Solid-state excitation/emission spectra of **1–6** at room temperature.

or abp as the bridging co-ligand, four coordination polymers **3**–**6** with different structural motifs were successfully constructed. These results indicate that although the available binding sites of H_2**ndc** and H_2**bdc** are very similar, their coordination chemistry and the role for involving supramolecular interactions are different; this can be ascribed to the electronic nature and the bulky skeleton of the extended π-conjugated system of the non-coordinating naphthalene group in **ndc**. This work, therefore, offers an opportunity to make a potential comparison of the corresponding coordination complexes constructed from two structurally related naphthalene- and benzene-based dicarboxylate tectons. Furthermore, from the viewpoint of ligand design, the present finding may provide an effective method for the design and preparation of new coordination architectures simply by changing the aromatic skeletons of different polycarboxyl systems.

Luminescent properties

Luminescent systems have attracted great attention because of their potential applications in chemical sensors and electroluminescent (EL) displays.[34] The synthesis of luminescent coordination complexes with well chosen ligands and d^{10} metal centers is an efficient method for producing new luminescence materials.[3d,11,35] The solid-state emission spectra of complexes **1–6** were investigated at room temperature (see Fig. 7). Excitation of the microcrystalline samples of **1–6** at 338, 346, 375, 344, 376, and 370 nm produce intense luminescence with the peak maxima at 382, 374, 478, 423, 415, and 414 nm, respectively. To further analyze the nature of these emission bands, the photoluminescent properties of H_2**ndc** as well as the 4bpy and abp co-ligands were also explored (see Fig. S15, ESI†). By comparing the locations and profiles of their excitation/emission peaks with complexes **1–6**, we can presume that these emissions are neither metal-to-ligand charge transfer (MLCT) nor ligand-to-metal charge transfer (LMCT) in nature, because the Ag(I) or Zn(II) ion with d^{10} configuration is difficult to oxidize or to reduce,[3d] and should mainly be ascribed to the intraligand $\pi\rightarrow\pi^*$ transitions of **ndc**, which are similar to those of the reported examples with naphthalene backbone.[11b] The different emissions in **1**/**3**/**5** or **2**/**4**/**6** should result from the introduction of different *N*-donor bridging co-ligands. In addition, compared with the emission peak of H_2**ndc**, the red shifts in **1** and **2** as well as blue shifts in **3–6** may result from the ligand chelating and/or bridging effect upon metal coordination, which can effectively modify the rigidity and conjugation, and then reduce the energy loss *via* a non-radiative pathway.[34] Further, the additional peak in the range of 450–500 nm for **5** is very weak and should be ascribed to background (see Fig. 7e).

Thermal stability

Thermogravimetric (TG) analyses were performed to explore the thermal stability of **1–6** (see Fig. S16, ESI†). Complex **1** remains intact until heating to 320 °C, and then suffers two consecutive weight losses to yield the Ag_2O residue (obsd: 51.98%; calcd: 53.90%) at about 650 °C (peaking at 341 and 613 °C). For **2**, a weight loss of 11.74% occurs in the range of 40–130 °C (peaking at 89 °C), corresponding to the loss of coordinated and lattice water molecules (calcd: 11.42%). The residue keeps thermally stable from 130 to 330 °C, and then shows a continuous weight loss of 56.65% from 325 to 800 °C (peaking at 387, 439, and 487 °C), revealing the decomposition of the coordination framework. In the temperature range of 40–180 °C, **3** suffers three consecutive weight losses of total 13.11% (peaking at 56 °C, 104 °C, and 159 °C), which may be attributed to the exclusion of lattice/coordinated water molecules and perchlorate ions (calcd: 13.23%). Then, four weight loss steps in the temperature range of 180–620 °C are observed, which can be ascribed to the loss of 4bpy and **ndc** ligands, and the final residue should be Ag_2O (obsd: 28.88%; calcd: 29.97%). The TG curve shows that **4** is thermally stable up to 260 °C, and then it starts to decompose quickly in three consecutive steps (peaking at 294, 354, and 441 °C). The weight loss of 63.10% observed from 260 to 500 °C can be assigned to the elimination of hydroxyl, 4bpy and partial **ndc**. With that, a continuous weight loss in the region 520–800 °C occurs with the final residue of 31.69%. The TGA curve of **5** exhibits five main steps of weight losses. The first weight loss of 6.52% appearing in the region 70–110 °C (peaking at 103 °C) can be attributed to the loss of lattice and coordinated aqua molecules (calcd: 6.34%). Then, the framework of **5** begins to decompose quickly in four consecutive steps (peaking at 160, 210, 310, and 602 °C) to produce the Ag_2O residue at *ca.* 630 °C (obsd: 25.70%; calcd: 27.19%). With regard to **6**, a weight loss of 8.93% occurs in the region 60–150 °C (peaking at 136 °C), which is attributed to the loss of coordinated and lattice water molecules (calcd: 8.84%). The dehydration is followed by a sharp weight loss (obsd: 62.19%) in the range of 150–480 °C (peaking at 272 and 462 °C) that can be assigned to the elimination of partial **ndc** and abp ligands, revealing the collapse of the coordination framework.

PXRD results

To confirm whether the crystal structures are truly representative of the bulk materials, powder X-ray diffraction (PXRD) experiments have been carried out for complexes **1–6**. The experimental and simulated PXRD patterns of the corresponding complexes are depicted in Fig. S17 (ESI†). Although the experimental patterns have a few unindexed diffraction lines and some peaks are slightly broadened in comparison with those simulated from the single crystal data, it still can be considered favorably that the bulk synthesized materials and the as-grown crystals are homogeneous for **1–6**.

Conclusion

We have successfully obtained a series of Ag(I) and Zn(II) coordination polymers exhibiting 1-D chain, 2-D layer (including a quite rare 5-connected topological net), and 3-D framework structures with a bulky naphthalene-based dicarboxylate ligand, 2,3-naphthalenedicarboxylate (**ndc**), incorporating different auxiliary *N*-donor bridging co-ligands. With the exception of auxiliary bridging spacers and metal ions, the results reveal that the naphthalene ring skeleton in **ndc**, showing an extended π-conjugated system and steric bulk, may play an important role in the formation of **1–6**, in comparison with those based on the structurally related **bdc** tecton. In addition, complexes **1–6** display strong blue emissions at room temperature, owing to the bulky naphthalene ring of **ndc**. Following this lead, the present work will prompt us to achieve more functional crystalline solids based on such a rational design strategy by using the dicarboxyl building blocks with larger conjugated π-systems (*e.g.* anthracene-2,3-dicarboxylic acid, H_2adc, see Chart 1). Further efforts in this perspective are in progress.

Acknowledgements

This work was supported by the National Natural Science Fund of China (Grant Nos. 20801049 and 21071129), Henan Outstanding Youth Science Fund (to C.S.L.), and Tianjin Normal University (to M.D.). We also thank Mr. X.-G. Yang for helping us to analyze the topological structures of **1** and **4**.

References

1 For examples: (*a*) A. N. Khlobystov, A. J. Blake, N. R. Champness, D. A. Lemenovskii, A. G. Majouga, N. V. Zyk and M. Schröder, *Coord. Chem. Rev.*, 2001, **222**, 155; (*b*) B.-H. Ye, M.-L. Tong and X.-M. Chen, *Coord. Chem. Rev.*, 2005, **249**, 545; (*c*) S. Natarajan and P. Mahata, *Chem. Soc. Rev.*, 2009, **38**, 2304.

2 (*a*) X.-H Bu, M.-L. Tong, H.-C. Chang, S. Kitagawa and S. R. Batten, *Angew. Chem., Int. Ed.*, 2004, **43**, 192; (*b*) H. A. Habib, A. Hoffmann, H. A. Hoppe, G. Steinfeld and C. Janiak, *Inorg. Chem.*, 2009, **48**, 2166.

3 (*a*) H. Hou, L. Li, Y. Zhu, Y. Fan and Y. Qiao, *Inorg. Chem.*, 2004, **43**, 4767; (*b*) S. Kitagawa and R. Matsuda, *Coord. Chem. Rev.*, 2007, **251**, 2490; (*c*) M. Dinca and J. R. Long, *Angew. Chem., Int. Ed.*, 2008, **47**, 6766; (*d*) Z. Chang, A.-S. Zhang, T.-L. Hu and X.-H. Bu, *Cryst. Growth Des.*, 2009, **9**, 4840.

4 (*a*) P. Mal, D. Schultz, K. Beyeh, K. Rissanen and J. R. Nitschke, *Angew. Chem., Int. Ed.*, 2008, **47**, 8297; (*b*) W.-C. Song, J.-R. Li, P.-C. Song, Y. Tao, Q. Yu, X.-L. Tong and X.-H. Bu, *Inorg. Chem.*, 2009, **48**, 3792.

5 (*a*) J.-C. Yao, W. Huang, B. Li, S. Gou and Y. Xu, *Inorg. Chem. Commun.*, 2002, **5**, 711; (*b*) S. G. Baca, Y. Simonov, M. Gdaniec, N. Gerbeleu, I. G. Filippova and G. A. Timco, *Inorg. Chem. Commun.*, 2003, **6**, 685; (*c*) E. Tang, Y.-M. Dai and S. Lin, *Acta Crystallogr., Sect. C: Cryst. Struct. Commun.*, 2004, **60**, m433; (*d*) Y.-G. Sun, D.-Z. Wei, E.-J. Gao and F. Ding, *Huaxue Xuebao*, 2004, **62**, 1362; (*e*) J. Zhang, Z.-J. Li, X.-Y. Cao and Y.-G. Yao, *J. Mol. Struct.*, 2005, **750**, 39; (*f*) A. Thirumurugan and C. N. R. Rao, *J. Mater. Chem.*, 2005, **15**, 3852; (*g*) Y. S. Song, B. Yan and Z.-X. Chen, *Appl. Organomet. Chem.*, 2006, **20**, 44; (*h*) W.-H. Li, F.-Q. Liu, X.-H. Pang and B.-R. Hou, *Acta Crystallogr., Sect. E: Struct. Rep. Online*, 2007, **63**, m1114; (*i*) W. Wu, J. Xie, Y. Xuan and N. Yuan, *Estestrvoispyt*, 2007, **23**, x241.

6 (*a*) X.-F. Li, Y. An and Y.-S. Yin, *Acta Crystallogr., Sect. E: Struct. Rep. Online*, 2008, **64**, m779; (*b*) Y.-L. Wang, Q.-Y. Liu, S.-L. Zhong and H.-P. Fu, *Chinese J. Struct. Chem.*, 2007, **26**, 1499; (*c*) D. R. Whitcomb and M. Rajeswaran, *J. Imaging Sci. Technol.*, 2003, **47**, 107; (*d*) D. R. Whitcomb and R. D. Rogers, *Inorg. Chim. Acta*, 1997, **256**, 263; (*e*) G. Smith, A. N. Reddy, K. A. Byriel and C. H. L. Kennard, *J. Chem. Soc., Dalton Trans.*, 1995, 3565; (*f*) M. Hedrich and H. Hartl, *Acta Crystallogr., Sect. C: Cryst. Struct. Commun.*, 1983, **39**, 1649; (*g*) M. B. Cingi, A. M. M. Lanfredi, A. Tiripicchio and C. M. Tiripicchio, *Acta Crystallogr., Sect. B: Struct. Crystallogr. Cryst. Chem.*, 1979, **35**, 312; (*h*) X. Gu and D. Xue, *Cryst. Growth Des.*, 2006, **6**, 2551.

7 (*a*) P.-K. Chen, Y.-X. Che, J.-M. Zheng and S. R. Batten, *Chem. Mater.*, 2007, **19**, 2162; (*b*) S. Horike, D. Tanaka, K. Nakagawa and S. Kitagawa, *Chem. Commun.*, 2007, 3395; (*c*) M. Du, X.-J. Jiang and X.-J. Zhao, *Inorg. Chem.*, 2007, **46**, 3984; (*d*) P. Ren, W. Shi and P. Cheng, *Cryst. Growth Des.*, 2008, **8**, 1097; (*e*) L. Zhang, Y.-Y. Qin, Z.-J. Li, Q.-P. Lin, J.-K. Cheng, J. Zhang and Y.-G. Yao, *Inorg. Chem.*, 2008, **47**, 8286; (*f*) H. Chun, H. Jung and J. Seo, *Inorg. Chem.*, 2009, **48**, 2043; (*g*) H. A. Habib, A. Hoffmann, H. A. Hoppe and C. Janiak, *Discussion of Faraday Soc.*, 2009, 1742.

8 (*a*) J. Hafizovic, M. Bjorgen, U. Olsbye, P. D. C. Dietzel, S. Bordiga, C. Prestipino, C. Lamberti and K. P. Lillerud, *J. Am. Chem. Soc.*, 2007, **129**, 3612; (*b*) H. Chun and J. Moon, *Inorg. Chem.*, 2007, **46**, 4371; (*c*) S.-M. Chen, J. Zhang and C.-Z. Lu, *CrystEngComm*, 2007, **9**, 390; (*d*) F.-K. Wang, S.-Y. Yang, R.-B. Huang, L.-S. Zheng and S. R. Batten, *CrystEngComm*, 2008, **10**, 1211; (*e*) R. Prajapati, L. Mishra, K. Kimura and P. Raghavaiah, *Polyhedron*, 2009, **28**, 600.

9 (*a*) F. Luo, Y.-X. Che and J.-M. Zheng, *Inorg. Chem. Commun.*, 2006, **9**, 1045; (*b*) J. Zhang, Y.-B. Chen, S.-M. Chen, Z.-J. Li, J.-K. Cheng and Y.-G. Yao, *Inorg. Chem.*, 2006, **45**, 3161; (*c*) L. Xu, E.-Y. Choi and Y.-U. Kwon, *Inorg. Chem. Commun.*, 2008, **11**, 1190; (*d*) J. Li, C. Ma, G. He and L. Qiu, *J. Coord. Chem.*, 2008, **61**, 251.

10 (*a*) M. A. Braverman and R. L. LaDuca, *CrystEngComm*, 2008, **10**, 117; (*b*) M.-X. Li, Z.-X. Miao, M. Shao, S.-W. Liang and S.-R. Zhu, *Inorg. Chem.*, 2008, **47**, 4481; (*c*) J.-D. Lin, J.-W. Cheng and S.-W. Du, *Cryst. Growth Des.*, 2008, **8**, 3345; (*d*) Y. Qi, Y. X. Che, F. Luo, S. R. Batten, Y. Liu and J. M. Zheng, *Cryst. Growth Des.*, 2008, **8**, 1654; (*e*) X.-G. Liu, L.-Y. Wang, X. Zhu, B.-L. Li and Y. Zhang, *Cryst. Growth Des.*, 2009, **9**, 3997; (*f*) D. S. Chowdhuri, A. Rana, M. Bera, E. Zangrando and S. Dalai, *Polyhedron*, 2009, **28**, 2131; (*g*) J. Yao, L. Wu, Y. Li and X. Mei, *J. Chem. Crystallogr.*, 2009, **39**, 246.

11 (*a*) C.-S. Liu, J.-J. Wang, L.-F. Yan, Z. Chang, X.-H. Bu, E. C. Sañudo and J. Ribas, *Inorg. Chem.*, 2007, **46**, 6299; (*b*) C.-S. Liu, X.-S. Shi, J.-R. Li, J.-J. Wang and X.-H. Bu, *Cryst. Growth Des.*, 2006, **6**, 656; (*c*) C.-S. Liu, P.-Q. Chen, Z. Chang, J.-J. Wang, L.-F. Yan, H.-W. Sun, X.-H. Bu, Z. Lin, Z.-M. Li and S. R. Batten, *Inorg. Chem. Commun.*, 2008, **11**, 159; (*d*) C.-S. Liu, E. C. Sañudo, L.-F. Yan, Z. Chang, J.-J. Wang and T.-L. Hu, *Transition Met. Chem.*, 2009, **34**, 51.

12 (*a*) D. Tanaka, S. Horike, S. Kitagawa, M. Ohba, M. Hasegawa, Y. Ozawa and K. Toriumi, *Chem. Commun.*, 2007, 3142; (*b*) T. Uemura, Y. Ono, K. Kitagawa and S. Kitagawa, *Macromolecules*, 2008, **41**, 87; (*c*) S. Ma, X.-S. Wang, C. D. Collier, E. S. Manis and H.-C. Zhou, *Inorg. Chem.*, 2007, **46**, 8499; (*d*) J.-J. Wang, C.-S. Liu, T.-L. Hu, Z. Chang, C.-Y. Li, L.-F. Yan, P.-Q. Chen, X.-H. Bu, Z.-M. Li, Q. Wu, L.-J. Zhao, Z. Wang and X.-Z. Zhang, *CrystEngComm*, 2008, **10**, 681; (*e*) C.-S. Liu, Z. Chang, J.-J. Wang, L.-F. Yan, X.-H. Bu and S. R. Batten, *Inorg. Chem. Commun.*, 2008, **11**, 889; (*f*) C.-S. Liu, M. Hu, S.-T. Ma, Q. Zhang, L.-M. Zhou, L.-J. Gao and S.-M. Fang, *Aust. J. Chem.*, 2010, **63**, 463.

13 (*a*) H. Chun, D. N. Dybtsev, H. Kim and K. Kim, *Chem.–Eur. J.*, 2005, **11**, 3521; (*b*) X.-J. Zheng, L.-P. Jin, S. Gao and S.-Z. Lu, *New J. Chem.*, 2005, **29**, 798; (*c*) J. Y. Lu and V. Schauss, *CrystEngComm*, 2002, **4**, 623; (*d*) N. Shan, A. D. Bond and W. Jones, *Tetrahedron Lett.*, 2002, **43**, 3101; (*e*) J. F. Bickley, R. P. Bonar-Law, C. Femoni, E. J. MacLean, A. Steiner and S. J. Teat, *J. Chem. Soc., Dalton Trans.*, 2000, 4025; (*f*) R. P. Bonar-Law, T. D. McGrath, N. Singh, J. F. Bickley and A. Steiner, *Chem. Commun.*, 1999, 2457; (*g*) T. K. Maji, M. Ohba and S. Kitagawa, *Inorg. Chem.*, 2005, **44**, 9225.

14 (*a*) H. R. Moon, N. Kobayashi and M. P. Suh, *Inorg. Chem.*, 2006, **45**, 8672; (*b*) K. O. Kongshaug and H. Fjellvag, *Solid State Sci.*, 2002, **4**, 443; (*c*) R. E. Marsh, *Acta Crystallogr., Sect. B: Struct. Sci.*, 2004, **60**, 252; (*d*) H.-F. Zhu, J. Fan, T. Okamura, W.-Y. Sun and N. Ueyama, *Cryst. Growth Des.*, 2005, **5**, 289.

15 (*a*) L.-F. Chen, J. Zhang, L.-J. Song and Z.-F. Ju, *Inorg. Chem. Commun.*, 2005, **8**, 555; (*b*) P. Wang, C. N. Moorefield, M. Panzer and G. R. Newkome, *Chem. Commun.*, 2005, 4405; (*c*) R. K. B. Nielsen, K. O. Kongshaug and H. Fjellvag, *Solid State Sci.*, 2006, **8**, 1237.

16 S. Martinez-Vargas, S. Hernandez-Ortega, R. A. Toscano, D. Salazar-Mendoza and J. Valdes-Martinez, *CrystEngComm*, 2008, **10**, 86.

17 E. V. Brown and G. R. Granneman, *J. Am. Chem. Soc.*, 1975, **97**, 621.

18 Bruker AXS, *SAINT Software Reference Manual*, Madison: WI, 1998.

19 G. M. Sheldrick, *SADABS, Siemens Area Detector Absorption Corrected Software*, University of Göttingen: Germany, 1996.

20 G. M. Sheldrick, *SHELXTL NT Version 5.1*. Program for Solution and Refinement of Crystal Structures, University of Göttingen: Germany, 1997.

21 (*a*) G. Wilkinson, R. D. Gillard and J. A. McCleverty, (ed.), (*Comprehensive Coordination Chemistry*, vol. 5, Pergamon, Oxford, 1987; (*b*) K. Nakamoto, *Infrared and Raman Spectra of Inorganic and Coordination Compounds*, John Wiley & Sons: New York, 1986.

22 (*a*) G. B. Deacon and R. J. Phillips, *Coord. Chem. Rev.*, 1980, **33**, 227; (*b*) M. Du, Z.-H. Zhang, X.-J. Zhao and Q. Xu, *Inorg. Chem.*, 2006, **45**, 5785.

23 (*a*) A. G. Orpen, L. Brammer, F. H. Allen, O. Kennard, D. G. Watson and R. Taylor, *J. Chem. Soc., Dalton Trans.*, 1989, S1; (*b*) M. O'Keeffe and N. E. Brese, *J. Am. Chem. Soc.*, 1991, **113**, 3226.

24 S.-L. Zheng, M.-L. Tong, S.-D. Tan, Y. Wang, J.-X. Shi, Y.-X. Tong, H. K. Lee and X.-M. Chen, *Organometallics*, 2001, **20**, 5319.

25 (*a*) P. Pyykkö, *Chem. Rev.*, 1997, **97**, 597; (*b*) M.-L. Tong, X.-M. Chen, B.-H. Ye and L.-N. Ji, *Angew. Chem., Int. Ed.*, 1999, **38**, 2237.

26 (*a*) A. F. Wells, *Three-Dimensional Nets and Polyhedra*, Wiley-Interscience, New York, 1977; (*b*) L. Carlucci, G. Ciani and D. M.

Proserpio, *Coord. Chem. Rev.*, 2003, **246**, 247; (*c*) M. O'Keeffe, M. A. Peskov, S. J. Ramsden and O. M. Yaghi, *Acc. Chem. Res.*, 2008, **41**, 1782.

27 (*a*) H. L. Sun, B. Q. Ma, S. Gao and S. R. Batten, *Cryst. Growth Des.*, 2005, **5**, 1331; (*b*) D. L. Long, A. J. Blake, N. R. Champness, C. Wilson and M. Schröder, *J. Am. Chem. Soc.*, 2001, **123**, 3401; (*c*) G. Yang, R. G. Raptis and P. Šafář, *Cryst. Growth Des.*, 2008, **8**, 981; (*d*) I. A. Baburin and V. A. Blatov, *Acta Crystallogr., Sect. B: Struct. Sci.*, 2007, **63**, 791; (*e*) C. Borel, M. Ghazzali, V. Langer and L. Öhrström, *Inorg. Chem. Commun.*, 2009, **12**, 105; (*f*) G.-H. Wang, Z.-G. Li, H.-Q. Jia, N.-H. Hu and J.-W. Xu, *Cryst. Growth Des.*, 2008, **8**, 1932; (*g*) M. R. Montney, S. M. Krishnan, N. M. Patel, R. M. Supkowski and R. L. LaDuca, *Cryst. Growth Des.*, 2007, **7**, 1145; (*h*) O. Delgado-Friedrichs, M. D. Foster, M. O'Keeffe, D. M. Proserpio, M. M. Treacy and O. M. Yaghi, *J. Solid State Chem.*, 2005, **178**, 2533.

28 (*a*) X. W. Wang, Y. R. Dong, Y. Q. Zheng and J. Z. Chen, *Cryst. Growth Des.*, 2007, **7**, 613; (*b*) R. J. Hill, D. L. Long, P. Hubberstey, M. Schröder and N. R. Champness, *J. Solid State Chem.*, 2005, **178**, 2414; (*c*) R. J. Hill, D. L. Long, M. S. Turvey, A. J. Blake, N. R. Champness, P. Hubberstey, C. Wilson and M. Schröder, *Chem. Commun.*, 2004, 1792; (*d*) L. Pan, N. Ching, X. Y. Huang and J. Li, *Chem. Commun.*, 2001, 1064.

29 (*a*) RCSR (Reticular Chemistry Structure Resource) with an associated website: http://rcsr.anu.edu.au/; (*b*) EPINET: S. T. Hyde, O. Delgado-Friedrichs, S. J. Ramsden and V. Robins, *Solid State Sci.*, 2006, **8**, 740 website: http://epinet.anu.edu.au; (*c*) V. A. Blatov, TOPOS, *A Multipurpose Crystallochemical Analysis with the Program Package*Samara State University, Russia, 2004.

30 C. Janiak, *J. Chem. Soc., Dalton Trans.*, 2000, 3885 and references therein.

31 G. R. Desiraju and T. Steiner, *The Weak Hydrogen Bond in Structural Chemistry and Biology*, Oxford University Press, Oxford. 1999.

32 For C–H···π interactions, please see: (*a*) M. Nishio, Y. Umezawa, K. Honda, S. Tsuboyama and H. Suezawa, *CrystEngComm*, 2009, **11**, 1757; (*b*) M. Nishio, M. Hirota and Y. Umezawa, A comprehensive monograph *The CH/π Interaction Evidence, Nature, and Consequences*, Wiley-VCH: New York, 1998, For more detailed information, please also refer to a website established by M. Nishio, http://www.tim.hi-ho.ne.jp/dionisio/.

33 (*a*) A. L. Spek, PLATON, *A Multipurpose Crystallographic Tool*, Utrecht University: Utrecht, The Netherlands, 2005; (*b*) A. L. Spek, *J. Appl. Crystallogr.*, 2003, **36**, 7; (*c*) A. L. Spek, *Acta Crystallogr., Sect. D: Biol. Crystallogr.*, 2009, **65**, 148.

34 (*a*) H. Yersin and A. Vogler, *Photochemistry and Photophysics of Coordination Compounds*; Springer: Berlin, 1987; (*b*) B. Valeur, *Molecular Fluorescence: Principles and Applications*, Wiley-VCH: Weinheim, Germany, 2002.

35 (*a*) E. Cariati, X. Bu and P. C. Ford, *Chem. Mater.*, 2000, **12**, 3385; (*b*) D. M. Ciurtin, N. G. Pschirer, M. D. Smith, U. H. F. Bunz and H.-C. zur Loye, *Chem. Mater.*, 2001, **13**, 2743.